



HAL
open science

Observational investigation of mass loss of M supergiants

E. Josselin, J. A. D. L. Blommaert, M. A. T. Groenewegen, A. Omont, F. L. Li

► **To cite this version:**

E. Josselin, J. A. D. L. Blommaert, M. A. T. Groenewegen, A. Omont, F. L. Li. Observational investigation of mass loss of M supergiants. *Astronomy and Astrophysics - A&A*, 2000, 357, pp.225-232. hal-04110363

HAL Id: hal-04110363

<https://hal.science/hal-04110363>

Submitted on 6 Jun 2023

HAL is a multi-disciplinary open access archive for the deposit and dissemination of scientific research documents, whether they are published or not. The documents may come from teaching and research institutions in France or abroad, or from public or private research centers.

L'archive ouverte pluridisciplinaire **HAL**, est destinée au dépôt et à la diffusion de documents scientifiques de niveau recherche, publiés ou non, émanant des établissements d'enseignement et de recherche français ou étrangers, des laboratoires publics ou privés.

Observational investigation of mass loss of M supergiants^{*,**}

E. Josselin^{1,2}, J.A.D.L. Blommaert³, M.A.T. Groenewegen⁴, A. Omon², and F.L. Li⁵

¹ Observatorio Astronómico Nacional, IGN, Apartado 1143, 28800 Alcalá de Henares, Spain

² Institut d'Astrophysique de Paris, CNRS, 98bis Boulevard Arago, 75014 Paris, France

³ ISO Data Centre, Astrophysics Division, Space Science Department of ESA, Villafranca, P.O. Box 50727, 28080 Madrid, Spain

⁴ Max-Planck-Institut für Astrophysik, Karl-Schwarzschild-Strasse 1, 85740 Garching, Germany

⁵ Université Paris VII Denis Diderot, 2 place Jussieu, 75251 Paris Cedex 05, France

Received 14 October 1999 / Accepted 29 February 2000

Abstract. We present the analysis of infrared photometry and millimeter spectroscopy of a sample of 74 late-type supergiants. These observations are particularly suitable to study the mass loss and the circumstellar envelopes of evolved massive stars. In particular, we quantify the circumstellar infrared excess, the relation of mass loss with stellar properties, using the K -[12] colour index as mass-loss indicator. We do not find any clear correlation between mass loss rate and luminosity. We also show that the K -band magnitude is a simple luminosity indicator, because of the relative constancy of the K -band bolometric correction.

Key words: stars: circumstellar matter – stars: mass-loss – stars: supergiants – infrared: stars

1. Introduction

Red supergiants represent a key-phase in the evolution of massive ($10 \lesssim M_{\text{init}} \lesssim 40 M_{\odot}$) stars, preceding Wolf-Rayet stars and/or supernovae. A good knowledge of their properties is necessary to compute reliable stellar evolutionary tracks and population synthesis models. For example, they are expected to represent the main $2 \mu\text{m}$ emitters in the central regions of active galaxies (e.g. Devereux 1989). Furthermore, because of mass loss during this phase, they play an important role in the chemical enrichment of the interstellar medium. Finally, thanks to their short lifetime and high luminosity, they can be used as tracers of galactic structure like spiral arms. As their luminosity peaks in the near-infrared, they are particularly suitable to probe regions affected by high interstellar extinction. Basic characteristics of these objects are summarized in Table 1.

The problem of mass loss of massive stars is very complex. Although circumstellar shells in expansion around supergiants

Table 1. Characteristics of red supergiants of our Galaxy and Magellanic Clouds (from Humphreys 1986).

Spectral Type	K, M
Effective temperature	$< 4000 \text{ K}$
Luminosity	$10^4\text{-}5 \cdot 10^5 L_{\odot}$
Mass	$10\text{-}50 M_{\odot}$
Radius	$300\text{-}2000 R_{\odot}$
Mass-loss rates	$10^{-7}\text{-}10^{-4} M_{\odot}/\text{yr}$

have been detected a long time ago (see e.g. Adams & MacCormack 1935, for $\alpha \text{ Ori}$ and $\alpha \text{ Sco}$), the understanding of mass loss in massive stellar evolution is still lacking. A better understanding of the physics of this phenomenon may be the key to solve a number of outstanding problems in massive star evolution (see Langer & Heger 1998 for a recent review). Among these problems are the prediction of the observed blue-to-red supergiant ratio or the explanation of the blue colour of the progenitor of SN 1987 A (Woosley et al. 1987). Indeed, mass loss must play a key-role in the occurrence of the “blue loop” in the evolutionary track of evolved massive stars (Chiosi & Maeder 1986). Anyhow, according to theoretical studies, the uncertainty on the mass loss rate may be as high as a factor of 10 (Woosley et al. 1993). Indeed, the process of mass loss is poorly understood. Magnetic fields, κ -mechanism and acoustic waves have been successively invoked to explain it, but none of these theories is completely satisfactory. Effects of stellar rotation may also be important (Langer & Heger 1998). Observational constraints are then needed.

Because of their low effective temperature and the presence of a cold circumstellar envelope, infrared and radio observations are particularly adapted to the study of M supergiants. The present paper presents the analysis of infrared photometry and millimeter spectroscopy of a sample of 74 late-type supergiants.

2. Sample and observations

Humphreys (1978) presented a catalogue of over 1000 supergiants and bright O stars in OB associations, giving B and V magnitudes, spectral types, distances and visible extinctions. From this catalogue, Stencel et al. (1989) selected all supergiants

Send offprint requests to: josselin@oan.es

* Based on observations collected at the European Southern Observatory, La Silla, Chile within program ESO 54.E-0914, and on observations collected with the IRAM 30m telescope.

** Tables A1 to A3 are only available in electronic form at the CDS via anonymous ftp to cdsarc.u-strasbg.fr (130.79.128.5) or via <http://cdsweb.u-strasbg.fr/Abstract.html>

Table 2. Characteristics of the filters used for the observations with IRAC1 (Lidman & Clements 1997) and TIMMI (Käuffel et al. 1992).

Filter	λ_c (μm)	$\Delta\lambda$ (μm)
<i>J</i>	1.25	0.30
<i>H</i>	1.65	0.30
<i>K</i>	2.20	0.40
<i>L'</i>	3.75	0.70
N1	8.39	0.96
N2	9.78	1.29
N3	12.56	1.41

Table 3. Characteristics of the detectors used for radio observations. Antenna temperatures have been converted to main-beam brightness temperatures according to $T_{\text{mb}} = T_{\text{A}}/\eta$ (η = forward efficiency/main-beam efficiency).

Line	Telescope	η	FWHM
CO(1–0)	IRAM	0.73	20.9''
	SEST	0.70	45.0''
CO(2–1)	IRAM	0.45	10.4''
HCN(1–0)	IRAM	0.73	27.0''
	SEST	0.75	57.0''
SO(6–5)	IRAM	0.48	10.9''
SiO(3–2)	SEST	0.68	40.0''
CS(3–2)	SEST	0.66	34.0''

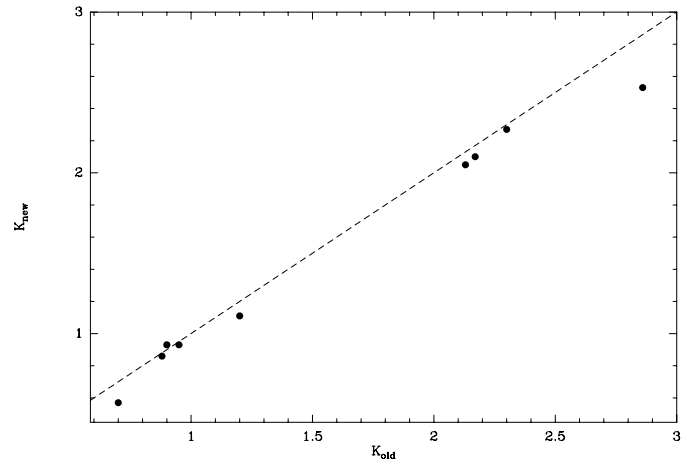
of spectral types F0 through M5, which represent a sample of 111 stars, of which 77 are of spectra type M. They tabulated IRAS data from which they examined the circumstellar shells of these objects.

Our sample is made up of 65 of these 77 M-type supergiants and 9 of the F to K supergiants from Stencel et al. (1989) catalogue, which were observed by ourselves or found in the literature. Their properties are given in Tables A1 and A2 in the appendix.

2.1. Infrared observations

Infrared photometry was found for 46 of the M-supergiants in the Gezari et al. (1993) catalogue (see Table A2).

Additional infrared photometry was obtained at ESO (La Silla, Chile) in February 1995 for 24 objects. Near-infrared photometry (*J*, *H*, *K* and *L'* bands) was obtained with IRAC1 at the 2.2m telescope, while mid-infrared photometry (N1, N2 and N3) was obtained with TIMMI at the 3.6m telescope. The characteristics of the filters are given in Table 2. The infrared standards were taken from van der Blik et al. (1996). The data were reduced using the Munich Image and Data Analysis System (MIDAS; ESO 1991). The precision of near-infrared photometry is about 2%. For TIMMI observations, the precision is lower (rms \sim 0.3 mag). The results of the observations are summarized in Table A1. No attempt was made to bring published data and our observations to a common photometric system. Given the supposed low variability of supergiants ($\Delta K \sim$ 0.2

**Fig. 1.** Comparison between published and our *K*-band observations. The plotted sources are, from left to right, HD 143183 (observed by Humphreys & Ney 1974), TV Gem (Kenyon 1988), HD 37536 (Lee 1970), BU Gem (Kenyon 1988), V396 Cen (Humphreys & Ney 1974), IC 2944 (Epchtein et al. 1987), HD 100930 (McGregor & Hyland 1984), CPD-57 3502 (McGregor & Hyland 1984) and CD-60 3621 (McGregor & Hyland 1984).

mag), the comparison with previous observations given in Fig. 1 shows that this should not affect our analysis.

The data have been corrected for interstellar extinction with the values of A_V given in Humphreys (1978) and A_λ/A_V values from Rieke & Lebofsky (1985).

2.2. Radio observations

Radio observations were performed in December 1994 with the IRAM–30m–telescope (Pico Veleta, Spain) and in February 1995 with the SEST (ESO, Chile). We observed the CO(1–0), CO(2–1), SiO($\nu=0, J=3-2$), HCN(1–0), SO(6–5) and CS(3–2) lines. The characteristics of the detectors are given in Table 3. Observations at SEST and at IRAM were done in position-switching mode, with a throw of $\sim 2'$ in both cases. The data were reduced using the Continuum and Line Analysis Simple Software (CLASS; Grenoble Observatory and IRAM).

The detection rate of molecular lines toward red supergiants is very low. Apart from the case of VY CMa, only the CO(2–1) and SiO(3–2) lines have been detected in a few objects. The parameters of radio observations are detailed in Table A3 in the appendix. Two objects we did not observe were previously detected in molecular lines: TV Gem (CO(1–0); Heske 1990) and HD 143183 (SiO($\nu=1,2-1$); Haikala et al. 1994).

3. Analysis

The colour-colour diagrams obtained by combining near-infrared photometry with optical magnitudes given by Humphreys (1978) and IRAS data are shown in Fig. 2. The [12] magnitude is calculated from the 12 μm IRAS flux:

$$[12] = -2.5 \times \log(S_{12}/28.3)$$

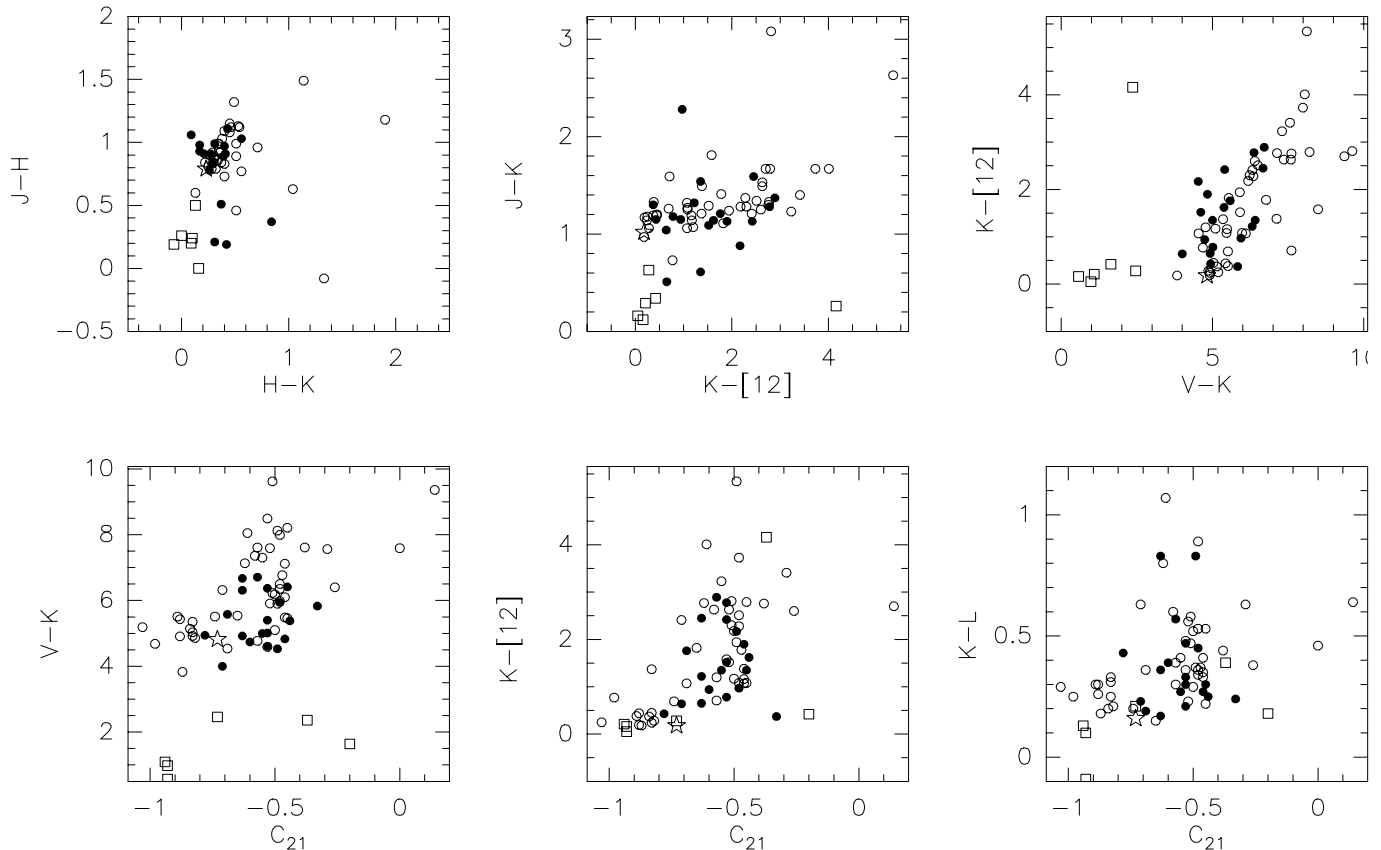


Fig. 2. Colour-colour diagrams for the objects studied in this paper. Open circles correspond to previous observations (data and references in Table A2), filled circles to our observations (data in Table A1), squares to F to K supergiants (Tables A1 and A2), and the star symbol to the model of a M1 I supergiant without circumstellar envelope (Fluks 1998).

(see IRAS Explanatory Supplement). The C_{21} colour is defined as

$$C_{21} = \log(12 \times S_{25}) / (25 \times S_{12})$$

The observed colours are compared to the ones obtained for a synthetic spectrum of a M1 I supergiant without circumstellar shell (Fluks 1998; star symbol in Fig. 2).

3.1. Mass loss of massive stars

Mass-loss rates can in principle be estimated from the circumstellar infrared ($\lambda > 1 \mu\text{m}$) excess generated by the presence of the circumstellar envelope. The comparison between observed spectral energy distribution (SED) and the photospheric spectrum of Fluks (1998) shows that this infrared excess represents at most about 20% of the total energy radiated and becomes noticeable at $\lambda \gtrsim 3\text{-}4 \mu\text{m}$. This last fact may reflect a low dust condensation temperature and/or the rapid cooling and dilution of the envelope because of its high expansion velocity. We now discuss different methods to estimate mass-loss rates.

3.1.1. Estimations based on near- and mid-infrared data

If we follow the criterion from Stencel et al. (1989) who assume a colour index $V - K > 6$ for mass-losing objects, about half

of the sources in our sample experience noticeable mass loss. This criterion corresponds to $K-[12] \gtrsim 1.5$ (see Fig. 2), or $L-[12] \gtrsim 1$. The photospheric spectrum of a star of spectral type M1 I (Fluks 1998) gives $V - K = 4.82$, $K-[12] = 0.18$, and $L-[12] = 0.02$, so that the criterion in Stencel et al. may be a bit conservative, in particular for the bluer objects. Furthermore, as shown above, the K -band emission seems to be essentially photospheric. Thus, we expect that the $K-[12]$ colour is a better indicator of mass loss. The sensitivity of the IRAS-12 μm band to the dust composition (silicate and SiC bands) must not affect the results, as all supergiants are oxygen-rich, as confirmed by LRS types (Tables A1 and A2). Only two objects are puzzling, AD Per and HD 37536, which display LRS types typical of carbon-rich circumstellar material (44 and 43, respectively). For both of them, the LRS spectra are noisy and the dust emission band is weak, so that they may have been misclassified (see Omont et al. 1993a for a discussion on such misclassifications).

Another colour, the IRAS C_{21} colour, is also often used to estimate mass-loss rates, in particular for AGB stars, as it is considered as a good indicator of circumstellar opacity. Fig. 2 shows that it displays little correlation with $K-[12]$. In particular, at $C_{21} \simeq -0.5$, the $K-[12]$ colour displays a large dispersion. This could be linked with different conditions of dust condensations in AGB stars and red supergiants or smaller extent of

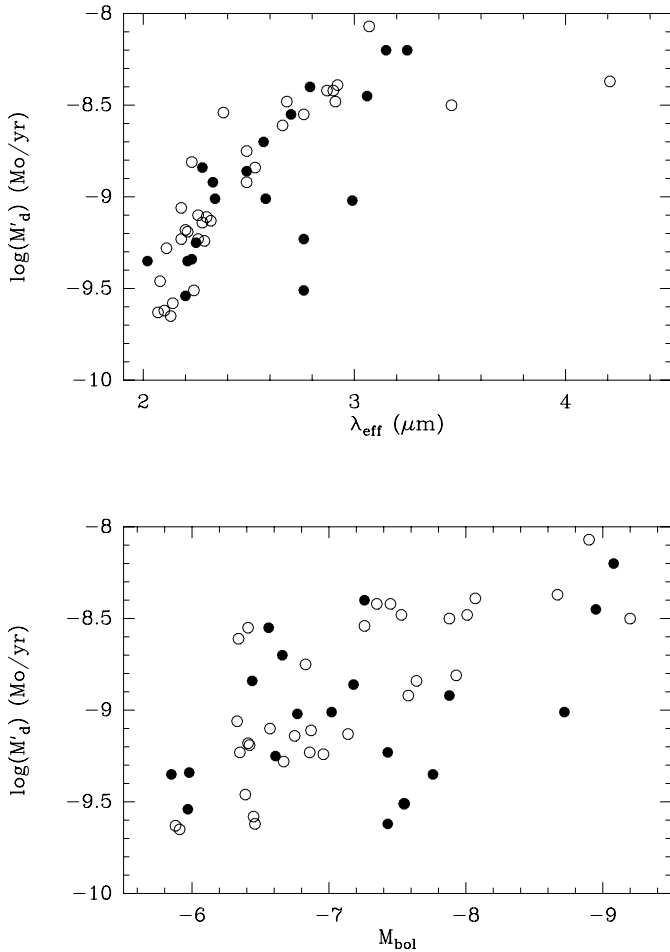


Fig. 3. Dust mass-loss rate (derived from the $K-[12]$ colour) as a function of the bolometric magnitude and effective wavelength. Same symbols as in Fig. 2.

the envelope. By the way, also Habing in his review (1996) indicates that C_{21} is not such a good indicator of mass loss (for AGB stars), especially for small mass loss rates ($< 10^{-6} M_{\odot} \text{ yr}^{-1}$).

The question of the use of the $K-[12]$ colour to estimate dust mass-loss rates (\dot{M}_d) has already been addressed for AGB stars by Whitelock et al. (1994). Before applying the relation they found between \dot{M}_d and $K-[12]$, we modified it to take into account the average difference of expansion velocities: 10 km s^{-1} for AGB stars, according to Whitelock et al. (1994), 25 km s^{-1} for +supergiants, assuming a linear dependence between \dot{M}_d and v_{exp} (Jura 1986). This gives

$$\log(\dot{M}_d/M_{\odot} \text{ yr}^{-1}) = 0.57 \times (K - [12]) - 9.95$$

The adopted value for v_{exp} , average of the values found from our radio observations (see Sect. 3.3), also corresponds to values observed for infrared supergiants, i.e. those who experience stronger mass loss (see Josselin et al. 1998).

The reliability of the obtained values of \dot{M}_d was checked with detailed radiative transfer calculations with the model of Groenewegen (1993) for the subsample of M1 supergiants. This

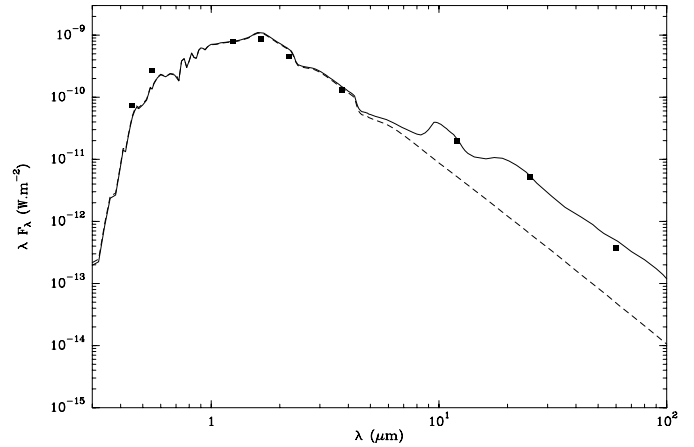


Fig. 4. Comparison between the observed spectral energy distribution (dots for the bands B , V , J , H , K , L , IRAS-12 μm , IRAS-25 μm and IRAS-60 μm), the photospheric spectrum (Fluks 1998; dashed line) and the result of radiative transfer for BU Gem with $\dot{M}_d = 7 \times 10^{-10} M_{\odot}/\text{yr}$ (solid line).

choice is justified by the availability of a stellar synthetic spectrum of this spectral type (Fluks 1998), preventing us from using a simple blackbody approximation, much less reliable, and the fact that a large range of \dot{M}_d is met in this subsample. The main free parameters are the mass-loss rate, the expansion velocity (when not measured in radio) and the dust condensation temperature. The program then gives a SED to be compared with the observed one and the dust optical depth ($\tau_{\lambda} \sim \dot{M}/R_{\text{in}}v_{\text{exp}}$, where R_{in} is the inner radius of the circumstellar envelope). Mass-loss rates derived in this way are consistent with those derived from the $(K-[12], \dot{M}_d)$ relation, within a factor of 2. Fig. 4 shows an example of the spectral energy distribution of a M1 supergiant of our sample together with the synthetic stellar spectrum of the same spectral type and the result of the radiative transfer calculation.

The values obtained for \dot{M}_d are compared to the absolute bolometric magnitude (when a distance modulus is available) and to an “effective” wavelength, as shown in Fig. 3. The absolute bolometric magnitude was obtained by integrating with a cubic spline the emission from B -band to IRAS-60 μm band, and the effective wavelength is defined as $\lambda_{\text{eff}} = (\int \lambda F_{\lambda})/(\int F_{\lambda})$.

The nice correlation found between \dot{M}_d and λ_{eff} (Fig. 3) is not surprising, as $K-[12]$ and λ_{eff} are both indicators of the opacity of the envelope. More interesting is the fact that there is essentially no correlation between \dot{M}_d and M_{bol} , over a relatively large range of luminosity (~ 3 mag). As evolutionary tracks without rotation predict an evolution at almost constant luminosity, this could also indicate that mass loss is independent of the initial mass of the star. However, a distribution of rotation rates would induce a spread in main sequence luminosities (Langer & Heger 1998), making this deduction uncertain. No correlation appears if we separate the different spectral subtypes, indicating that Reimers (1975) formula ($\dot{M} \propto L/(g \times R) \propto (L \times R)/M$) may not apply to red supergiants. Anyhow, the values of \dot{M}_d may be subject to large uncertainties. For example, the mass

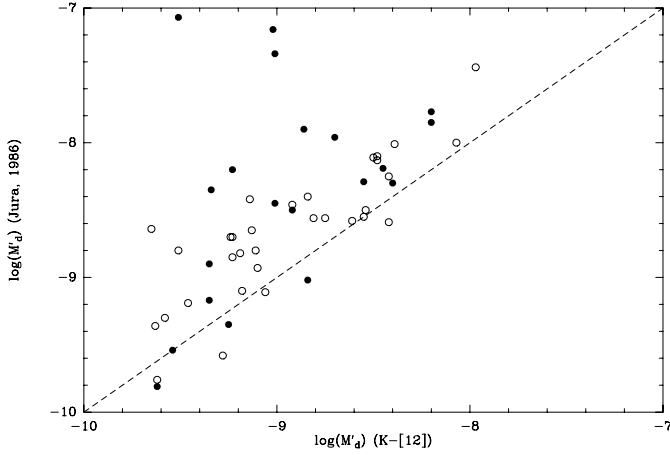


Fig. 5. Comparison between dust mass-loss rates estimated from the $(K-[12])$ colour and from Jura (1986) formula.

loss estimators we used assume spherical symmetry, which is probably not the case at least for some objects (see e.g. Kafatos & Michalitsianos 1979, for the cases of S Per, TV Gem, α Sco, BI Cyg, BC Cyg, RW Cyg, μ Cep and VV Cep).

The lack of correlation between \dot{M}_d and the luminosity is in contradiction with what is expected for evolved low-mass stars and it is in opposition with some theoretical works, such those about Magellanic Clouds supergiants (see Salasnich et al. 1999, and references therein). In this latter case, the (\dot{M}, L) relation is a synthesis between (\dot{M}, period) and (period, L) relations. But many galactic M supergiants are known to be irregular variables. Such a relation is then not relevant (see also the discussion about VY CMA in Sect. 3.3). In fact, this model, as many other ones, is an extrapolation of those about AGB stars, assuming identical processes, while pulsational properties are known to be different.

It is worth recalling here that our sample is essentially made of supergiants with optically thin envelopes. The results given above may then not be extrapolated to objects during an eventual “superwind” phase.

3.1.2. Other estimators

Mass-loss rates of AGB stars are commonly estimated from the IRAS $60 \mu\text{m}$ flux S_{60} , assuming that this reflects the dust emission (Jura 1986), or from the the CO(1-0) line intensity, assuming that all carbon is in form of CO in an oxygen-rich medium, within the limits of photodissociation by interstellar UV radiation (Knapp & Morris 1985; Loup et al. 1993).

Fig. 5 shows the comparison between the estimation of \dot{M}_d based on the $(K-[12])$ colour, as detailed above, and the one based on Jura formula:

$$\dot{M}_d = 2.1 \times 10^{-9} \frac{v_{\text{exp}}}{10 \text{ km/s}} \left(\frac{d}{1 \text{ kpc}} \right)^2 \frac{\lambda_{\text{eff}}}{1 \mu\text{m}} \frac{10^4 L_{\odot}}{S_{60}} M_{\odot}/\text{yr}$$

(where d is the distance, given by Humphreys 1978, and λ_{eff} is the mean wavelength of radiation of dust). It appears that the last one is systematically greater than the first one. First of all,

Table 4. Gas mass-loss rates estimates based on CO(2-1) emission and gas-to-dust ratio (χ).

Object	$\dot{M}_g(\text{CO})$ (M_{\odot}/yr)	χ
S Per	1.4×10^{-6}	86
W Per	9.0×10^{-7}	167
VY CMA	1.6×10^{-5}	77
μ Cep	9.1×10^{-8}	65
PZ Cas	8.3×10^{-6}	776

one should keep in mind that Jura’s formula was established for carbon stars. The mass opacity is the main parameter which takes into account the effects of different dust compositions. The above formula assumes $\kappa(60 \mu\text{m}) = 150 \text{ cm}^2 \text{ g}^{-1}$. If this value is not appropriate, this would result in a systematic difference between both mass-loss rates estimates, but it cannot explain the observed dispersion. More important, as the sample considered here contains mainly objects with optically thin envelopes, the $60 \mu\text{m}$ flux is dominated by the stellar contribution, as demonstrated by Groenewegen & de Jong (1998). Following their calculation (their Fig. 4), the stellar $60 \mu\text{m}$ flux would represent more than half of the total flux in this band for at least 20% of the objects in our sample. Furthermore, regarding their low galactic latitude, interstellar contamination in the far-infrared may be not negligible. Altogether, the use of Jura (1986) formula with the assumption that S_{60} only traces the circumstellar dust shell must lead to an overestimation of the dust mass-loss rate, which explains the observed discrepancy in Fig. 5.

We also estimated the gas mass-loss rate from CO emission for the five objects which were detected. From Olofsson et al. (1993),

$$\dot{M}_g = 1.4 \frac{T_{\text{mb}} v_{\text{exp}}^2 d^2 B^2}{2 \times 10^{19} f_{\text{CO}}^{0.85} s(J)} M_{\odot}/\text{yr}$$

where T_{mb} is the main beam temperature in Kelvin of the (J,J-1) transition, d the distance in pc, B the FWHM size of the telescope beam in arcsec (see values in Table 3), f_{CO} the CO abundance relative to H_2 (we took $f_{\text{CO}} = 5 \times 10^{-4}$, a typical value for oxygen-rich stars) and $s(J)$ a correction factor. $s(J=1) = 1$ and $s(J=2)$ equals the ratio between the average integrated intensity ratio $I(J=2-1)/I(J=1-0)$ and the square of the beam width ratio at both frequencies. Estimates given in Table 4 are based on the (J=2-1) line. We adopted a value of 4 for the $I(J=2-1)/I(J=1-0)$ ratio, which corresponds to the optically thin limit and is in agreement with the upper limits found for the (J=1-0) line (see Sect. 3.3). One may note that a value of 5.5 is observed for VY CMA, the only object detected in both CO lines, but dilution effects and the fact that this object may be slightly resolved have to be taken into account before converting this ratio into the intrinsic one.

It is known that many supergiants have an active chromosphere which produces photodissociating ultraviolet radiation (see e.g. the case of α Ori, Glassgold & Huggins 1986). Then, considering that carbon is essentially in the form of CO, as assumed when taking a “standard” value of 5×10^{-4} for f_{CO} ,

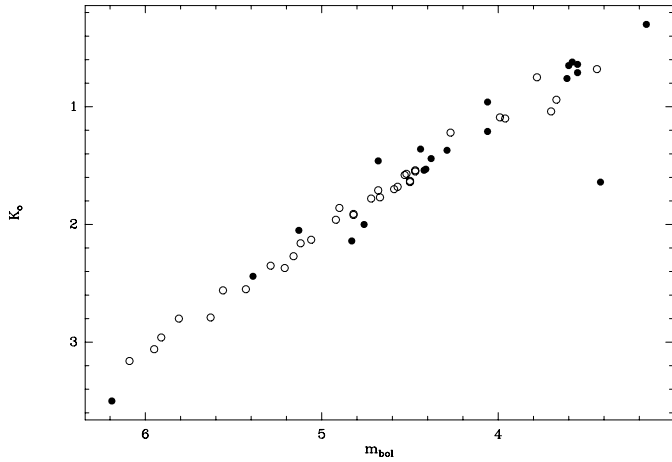


Fig. 6. Correlation between K -band and bolometric magnitudes (all magnitudes are corrected for interstellar extinction).

will lead to an under-estimation of the gas mass-loss rate (see Josselin et al. 1998 for other possible effects). Indeed, if we estimate the gas-to-dust ratio by comparing the values of \dot{M}_g with \dot{M}_d obtained from the $(K-[12])$ colour (Table 4), we obtain very low values, except for PZ Cas, compared with what is generally assumed for AGB stars ($\chi \sim 200$).

3.2. Indicator of luminosity and bolometric correction

The comparison between the bolometric magnitude and the K -magnitude, corrected for interstellar extinction, is shown in Fig. 6. A relation appears:

$$m_{\text{bol}} \simeq m_K - 3$$

similar to the relation found by Groenewegen (1997) for AGB stars. One object, HD 74180, shows strong departure from this relation. The weakness of its IRAS fluxes ($S_{25} = 2.81$ Jy, $S_{60} < 0.72$ Jy) makes uncertain the determination of the infrared luminosity.

Fig. 7 shows an example of a search for a possible dependence of the bolometric correction on the $(J - K)$ colour. It is zoomed on the $0.5 \leq (J - K) \leq 1.5$ interval, where most of the M-supergiants are concentrated (see Fig. 2). A general trend appears, but with a relatively weak correlation coefficient. The J -band contains many molecular bands (in particular CO and OH; see Lançon & Rocca-Volmerange 1992), which may be very sensitive to effective temperature and metallicity and thus explain the observed dispersion.

We also note that no star is brighter than $M_K = -12$ mag, or $M_{\text{bol}} = -9.5$ mag, as expected by Humphreys (1986). This limit has been explained by de Jager (1991) as a stability limit by dissipation of energy, preventing the most massive stars from reaching the M-type region.

3.3. Molecular content of the circumstellar envelopes

Regarding the large number of non-detections in Table A3, the molecular content of the envelopes of red supergiants appears

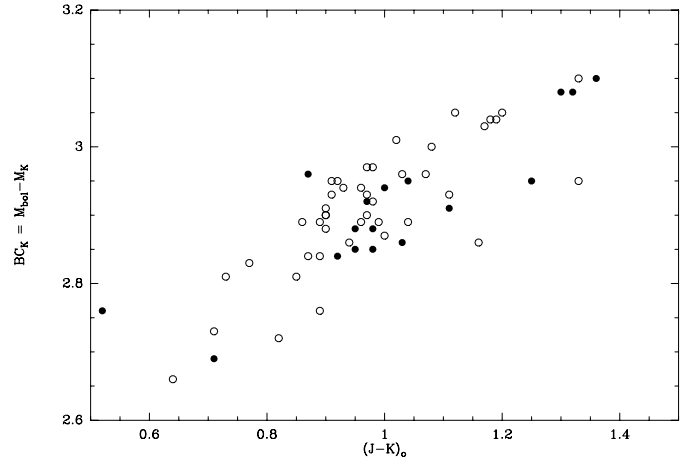


Fig. 7. Bolometric correction in the K -band versus $(J - K)$ (all magnitudes are corrected for interstellar extinction).

quite poor. Nevertheless, this low detection rate may be partly due to the low mass-loss rates measured in our sample. Among the rare detections, the CO(2-1) and SiO(3-2) are the most frequent. But because of their low galactic latitude, many CO and HCN observations are affected by interstellar lines, so limits on molecular abundances are difficult to derive.

Concerning CO, the observed ratios $I_{\text{CO}(2-1)}/I_{\text{CO}(1-0)}$ are greater than 4. This is characteristic of optically thin envelopes and suggests a radiative excitation of this molecule (see e.g. Groenewegen et al. 1997). Furthermore, these low opacities offer little protection against photodissociation of CO by chromospheric and/or interstellar UV radiations and then, explain at least partly the weakness of the CO lines.

The SiO($v=0, J=3-2$) thermal line is detected in VY CMa and EV Car. Furthermore the SiO($v=1, J=2-1$) maser line was detected in HD 143183 (Haikala et al. 1994). EV Car and HD 143183 are not detected in CO, so the circumstellar gas should be essentially in atomic form. Then, SiO emission may reveal very low depletion of Si on grains and/or eventually the occurrence of shocks in the inner envelopes, where SiO would be more protected against photodissociating radiation.

No object was detected in the CS(3-2) line and only one in the HCN(1-0) line (VY CMa, see hereafter). Both molecules may result from photochemical processes. Furthermore, when detected in O-rich circumstellar envelopes, the CS emission is always very weak (Omont et al. 1993b and references therein).

In all detections, the expansion velocities are relatively high ($\gtrsim 18$ km s $^{-1}$), compared to values usually observed for AGB stars. Radiation pressure is usually invoked to explain this gap, but the low surface gravity of supergiants combined with a large inner radius of the circumstellar envelope may be an alternative explanation.

3.3.1. VY CMa

A case of particular interest is VY CMa, which has been detected in four molecules: CO, HCN, SiO and SO. A striking point is the apparent large dispersion of the expansion velocity as a function

of the molecular line. This could reflect differences in signal-to-noise ratio. But if this is real, this probably indicates large inhomogeneities in the envelope, with the occurrence of rapidly expanding blobs in the internal envelope. Indeed, the largest observed value of v_{exp} correspond to SiO, which is believed to form closer to the star than CO. Furthermore, the molecular lines shown in Fig. A.1 have complex profiles, with multiple peaks. Then, the mass loss process is certainly not spherically symmetric, as already suggested from the VLA map of the OH 1612 MHz maser emission (Bowers et al. 1983), and not linked with radial pulsations: VY CMa is known as an irregular variable of small amplitude (type Lc, $\Delta V = 0.90$ mag), while the observed mass-loss rate is important ($\gtrsim 10^{-5} M_{\odot}/\text{yr}$). Stencel et al. (1989) already suggested that turbulent processes rather than regular pulsations may be at the origin of mass loss.

Concerning its circumstellar chemistry, as already stressed by Bujarrabal et al. (1994), the most striking point is the strength of the HCN(1-0) line in an O-rich medium. This molecule is probably the result of an active photochemistry, induced by either chromospheric or interstellar UV radiations (Nercessian et al. 1989).

3.4. F, G and K supergiants

Our subsample of yellow supergiants is too limited to draw out some definite conclusions. Furthermore, most of them are rather weak IRAS sources. Then, together with possible interstellar contamination because of the low galactic latitude of these objects, mid-infrared colours (Fig. 2) may be subject to quite large uncertainties.

Only one, namely HR 5171a, seems to have a relatively high mass-loss rate, from its K -[12] colour. But its near-infrared colours (e.g. $J - K$) are here again essentially photospheric. This is also one of the brightest sources, with a luminosity close to the Humphreys-de Jager limit ($M_{\text{bol}} \simeq -9.1$ mag). Then, it could also be one of the most massive stars in our sample. We tentatively detected SiO emission at the 2σ level at $V_{\text{LSR}} \simeq 41 \text{ km s}^{-1}$.

Because of no noticeable circumstellar infrared excess, the other objects may be on the blue-to-red evolution path, if we assume that *all* supergiants lose mass during the red phase.

4. Conclusion

From the analysis of infrared and millimeter observations of 74 late-type supergiants, we derived some interesting properties of massive stars and their circumstellar envelopes. We discussed the relation of infrared colour excess with mass loss, with the conclusion that the K -[12] colour may give a reasonably good estimate of the mass-loss rate as for AGB stars. No correlation between the dust mass-loss rate and the luminosity appears. Combined with possible strong inhomogeneities in the envelopes, as in the case of VY CMa, and the fact that most of red supergiants are irregular, low-amplitude variables, the mass loss process must not necessarily be linked to radial pulsations, and so could be different from that of AGB stars. Furthermore,

we confirmed that, as for AGB stars, the K -magnitude is a good luminosity indicator, since the K -bolometric correction remains rather constant for a wide range of parameters.

Acknowledgements. We are grateful to the ESO and IRAM (Pico Veleta) staff members for their assistance during the observations and to an anonymous referee for useful comments which improved the presentation of this paper. This research has made use of the Simbad database, operated at CDS, Strasbourg, France.

Appendix A: infrared and radio measurements

References

- Adams W.S., MacCormack E., 1935, ApJ 81, 119
 Bowers P.F., Johnston K.J., Spencer J.H., 1983, ApJ 274, 733
 Bujarrabal V., Fuente A., Omont A., 1994, A&A 285, 247
 Chiosi C., Maeder A., 1986, ARA&A 24, 329
 de Jager C., 1991, A&A 244, 131
 Devereux N.A., 1989, ApJ 346, 126
 Epchtein N., Le Bertre T., Lepine J.R.D., 1987, A&AS 71, 39
 Fluks M.A., 1998, Ph.D. Thesis, Univ. of Amsterdam, The Netherlands
 Frogel J.A., Persson S.E., Aaronson M., Matthews K., 1978, ApJ 220, 75
 Gezari D.Y., Schmitz M., Pitts P.S., Mead J.M., 1993, Catalog of Infrared Observations. NASA Ref. Pub. 1294
 Glassgold A.E., Huggins P.J., 1986, ApJ 306, 605
 Groenewegen M.A.T., 1993, Ph.D. Thesis, Univ. of Amsterdam, The Netherlands
 Groenewegen M.A.T., 1997, In: Garzón F., Epchtein N., Omont A., et al., (eds.) The Impact of Large Scale Near-IR Sky Surveys. Kluwer Acad. Pub., Dordrecht, p. 165
 Groenewegen M.A.T., Baas F., Blommaert J., Josselin E., Tilanus R.P.J., 1997, In: Shaver P.A. (ed.) Science with Large Millimetre Arrays. Springer Verlag, p. 286
 Groenewegen M.A.T., de Jong T., 1998, A&A 337, 797
 Habing H.J., 1996, A&AR 7, 97
 Haikala L.K., Nyman L.-Å., Forsstroem V., 1994, A&AS 103, 107
 Heske A., 1990, A&A 229, 494
 Humphreys R.M., 1986, In: Luminous stars and associations in Galaxies. IAU Symp. No. 116, p. 45
 Humphreys R.M., 1978, ApJS 38, 309
 Humphreys R.M., Ney E.P., 1974, ApJ 194, 623
 Hyland A.R., Becklin E.E., Neugebauer G., Wallerstein G., 1969, ApJ 158, 619
 Hyland A.R., Becklin E.E., Frogel J.A., Neugebauer G., 1972, A&A 16, 204
 IRAS Science Team, 1986, A&AS 65, 607
 Johnson H.L., 1965, Comm. Lunar and Planetary Lab. 3, 79
 Johnson H.L., Mendoza V.E.E., 1966, Ann. Ast. 29, 525
 Johnson H.L., Mitchell R.I., Iriarte B., Wisniewsk W.Z., 1966, Comm. Lunar and Planetary Lab. 4, 99
 Josselin E., Loup C., Omont A., et al., 1998, A&AS 129, 45
 Jura M., 1986, ApJ 303, 327
 Kafatos M., Michalitsianos A.G., 1979, ApJ 228, L115
 Kenyon S.J., 1988, AJ 96, 337
 Knapp G.R., Morris M., 1985, ApJ 292, 640
 Käußl H.U., Jouan R., Lagage P.O., et al., 1992, The Messenger 70, 67
 Lançon A., Rocca-Volmerange B., 1992, A&AS 96, 593
 Langer N., Heger A., 1998, IAU Symp. 190, p. 192
 Lee T.A., 1970, ApJ 162, 217

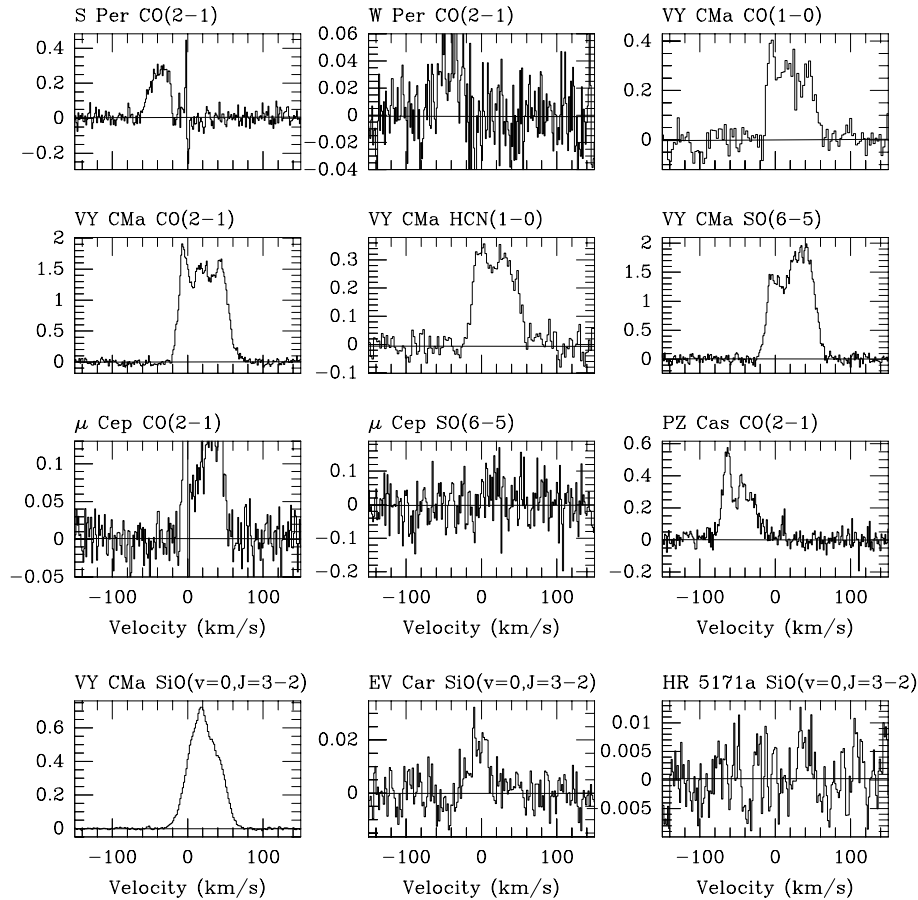


Fig. A.1. Spectra of the objects detected at IRAM.

Fig. A.2. Spectra of the objects detected at SEST.

Lidman C., Clements D., 1997, IRAC1 ESO Manual
 Loup C., Forveille T., Omont A., Paul J.F., 1993, *A&AS* 99, 291
 McGregor P.J., Hyland A.R., 1984, *ApJ* 277, 149
 Nercessian E., Omont A., Benayoun J.J., Guilloteau S., 1989, *A&A* 210, 225
 Ney E.P., Merrill K.M., 1980, AFGL-TR-80-0050
 Noguchi K., Kawara K., Kobayashi Y., et al., 1981, *PASJ* 33, 373
 Olofsson H., Eriksson K., Gustafsson B., Carlström U., 1993, *ApJS* 87, 267
 Omont A., Loup C., Forveille T., et al., 1993a, *A&A* 267, 515
 Omont A., Lucas R., Morris M., Guilloteau S., 1993b, *A&A* 267, 490
 Reimers D., 1975, *Mem. Soc. R. Sci. Liège*, 8, 369
 Rieke G.H., Lebofsky M.J., 1985, *ApJ* 288, 618
 Salasnich B., Bressan A., Chiosi C., 1999, *A&A* 342, 131
 Stencel R.E., Pesce J.E., Hagen Bauer W., 1989, *AJ* 97, 1120

Tapia M., Roth M., Costero R., Navarro S., 1984, *Rev. Mex. Astron. Astrofis.* 9, 65
 Tapia M., Roth M., Marraco H., Ruiz M.T., 1988, *MNRAS* 232, 661
 The P.S., Wesselius P.R., Janssen I.M.H.H., 1986, *A&AS* 66, 63
 Thomas J.A., Hyland A.R., Robinson G., 1973, *MNRAS* 165, 201
 van der Blik N.S., Manfroid J., Bouchet P., 1996, *A&AS* 119, 547
 van der Veen W.E.C.J., Habing H.J., 1988, *A&A* 194, 125
 Voelcker K., 1975, *A&AS* 22, 1
 Welch D.L., Wieland F., McAlary C.W., et al., 1984, *ApJS* 54, 547
 Whitelock P.A., Menzies J.W., Feast M.W., et al., 1994, *MNRAS* 267, 711
 Woosley S.E., Langer N., Weaver T.A., 1993, *ApJ* 411, 823
 Woosley S.E., Pinto P.A., Martin P.G., Weaver T.A., 1987, *ApJ* 318, 664